

# Universality and corrections to scaling in the ballistic deposition model

F. D. A. Aarão Reis

*Instituto de Física, Universidade Federal Fluminense, Avenida Litorânea s/n, 24210-340 Niterói Rio de Janeiro, Brazil*

(Received 17 January 2001; published 20 April 2001)

In order to analyze some controversies on the equivalence between ballistic deposition (BD) and the Kardar-Parisi-Zhang (KPZ) theory, we simulated the BD model in one and two dimensions. Effective exponents  $\beta_L$  were obtained in the growth regions, which were rigorously determined for various lengths  $L$ . Effective exponents  $\alpha_L$  were obtained from saturation widths in the steady-state regimes. In  $d=1$  we found  $\beta_L = \beta + AL^{-\lambda}$  and  $\alpha_L = \alpha + BL^{-\Delta}$ , with asymptotic exponents consistent with the KPZ values  $\beta=1/3$  and  $\alpha=1/2$ , and correction-to-scaling exponents  $0.2 \leq \lambda \leq 0.4$  and  $0.6 \leq \Delta \leq 0.8$ . These strong finite-size corrections explain the previous discrepancies between numerical estimates for BD and the exact KPZ results. In  $d=2$  we could only obtain reliable estimates of  $\alpha_L$ , which are consistent with KPZ values if finite-size corrections with  $\Delta \approx 0.4$  are considered.

DOI: 10.1103/PhysRevE.63.056116

PACS number(s): 05.50.+q, 05.40.-a

## I. INTRODUCTION

Ballistic deposition (BD) is one of the most interesting growth models for its large number of applications (see, e.g., Ref. [1] or recent papers [2–4]). In the simplest version of the model, at each unit of time a particle is released from a randomly chosen position above a  $d$ -dimensional substrate, follows a trajectory perpendicular to the surface, and sticks upon first contact with a nearest neighbor occupied site [5,6]. The resulting aggregate is porous, and has a rough surface which exhibits dynamic scaling behavior. Despite the intensive study of this model and its generalizations, the numerical values of critical exponents reported in several works are controversial, and the equivalence to the Kardar-Parisi-Zhang (KPZ) universality class is not clear.

When one studies surface properties, the main quantity of interest is the interface width of the deposit. In a surface of length  $L$  ( $L^d$  columns) at time  $t$ , it is usually defined as

$$W(L,t) = \left\langle \left[ \frac{1}{L^d} \sum_i (h_i - \bar{h})^2 \right]^{1/2} \right\rangle. \quad (1)$$

Here  $h_i$  is the height of column  $i$ , the bar over  $\bar{h}$  denotes a spatial average, and the brackets denote a configurational average, i.e., an average over many realizations of the noise. Alternatively, the interface width is defined by some authors as

$$\xi(L,t) = \left[ \left\langle \frac{1}{L^d} \sum_i (h_i - \bar{h})^2 \right\rangle \right]^{1/2}. \quad (2)$$

Although  $W$  and  $\xi$  have different values, they obey the same dynamic scaling relation

$$W \approx L^\alpha f(tL^{-z}). \quad (3)$$

Then, in the rest of this paper, any definition or discussion concerning  $W$  is also valid for  $\xi$ , except when the opposite is explicitly mentioned. The exponent  $\alpha$  in Eq. (3) describes the long-time behavior of the problem, when the interface width saturates at

$$W_\infty(L) \equiv W(L, t \rightarrow \infty) \sim L^\alpha. \quad (4)$$

On the other hand, at early times finite-size effects are weak, and the interface width increases as

$$W \sim t^\beta, \quad \beta = z/\alpha. \quad (5)$$

In order to present a hydrodynamic description of kinetic surface roughening, Kardar, Parisi, and Zhang [7] proposed the Langevin-type equation

$$\frac{\partial h}{\partial t} = \nu \nabla^2 h + \frac{\lambda}{2} (\nabla h)^2 + \eta(\vec{x}, t), \quad (6)$$

known as the KPZ equation. Here  $h$  is the height at position  $\vec{x}$  at time  $t$ ,  $\nu$  represents a surface tension,  $\lambda$  represents the ‘‘excess velocity,’’ and  $\eta$  is a Gaussian noise [1,7]. The solutions of the KPZ equation satisfy the scaling relation [Eq. (3)]. In  $d=1$  the exact values  $\beta=1/3$  and  $\alpha=1/2$  were obtained [7]. In  $d=2$ , numerical works gave  $\beta \approx 0.24$  and  $\alpha \approx 0.39$  [8,9], and a recent analytical work suggested the exact value  $\alpha=0.4$  [10].

Many discrete growth models are expected to be in the KPZ universality class. This conjecture was confirmed numerically with a high accuracy for various models, including the restricted solid-on-solid (RSOS) model of Kim and Kosterlitz [11] and some of its generalizations. The same is expected for BD. Indeed, a connection between BD and the KPZ equation was recently derived with analytical methods [12].

However, most numerical works on BD in  $d=1$  give estimates of exponent  $\beta$  smaller than the KPZ value [6,13–16]: the reported estimates range from  $\beta=0.30$  to 0.331 (central estimates, not including error bars). Moreover, to our knowledge all previous estimates of exponent  $\alpha$  are smaller than the KPZ value [6,13–15,17]: they range from  $\alpha=0.42$  to 0.47, and the error bars do not include  $\alpha=0.5$ . A summary of numerical data for the BD model is given in Ref. [15]. Although the quality of the random number generators may have been responsible for some deviations in previous works, as discussed by D’Souza *et al.* [17] the careful numerical simulations of those authors gave  $\alpha=0.45$  in  $d=1$ ,

which is still 10% smaller than the KPZ value. In  $d=2$  the situation is more difficult, because there is no exact calculation of critical exponents for both the KPZ equation and BD.

This scenario suggests that further numerical investigations are necessary to clarify the question of the universality class of BD, particularly in  $d=1$ . In this work, we present a systematic numerical study of BD that confirms that this model is in the KPZ universality class in  $d=1$ , and suggests the same for  $d=2$ . Simulations will be performed on lattices with  $L=64-L=16384$  in  $d=1$ , and lattices with  $L=16-L=1024$  in  $d=2$ . Combinations of simple random number generators will be used, but no bias associated with them is observed. Finite-size estimates of exponent  $\beta$  (effective exponents  $\beta_L$ ) will be obtained in the growth region, and finite-size estimates of exponent  $\alpha$  (effective exponents  $\alpha_L$ ) will be obtained from the saturation widths  $W_\infty(L)$ . In  $d=1$ , extrapolations of the effective exponents to  $L \rightarrow \infty$  will provide asymptotic estimates of  $\beta$  and  $\alpha$ , in good agreement with the KPZ values, and will suggest the presence of strong corrections to scaling. Thus this work is important not only for confirming the universality class of BD but also for estimating finite-size corrections to Eqs. (4) and (5). In  $d=2$ , less accurate results for  $\alpha_L$  will be obtained but, including such corrections, they are also consistent with numerical estimates for the KPZ universality class.

The rest of this paper is organized as follows. In Sec II we present the simulation results for  $d=1$ , the methods to calculate effective exponents, and the asymptotic estimates of  $\beta$  and  $\alpha$ . In Sec. III we present the simulations' results for  $d=2$ , and obtain estimates of exponent  $\alpha$ . In Sec. IV we summarize our results and present our conclusions.

## II. BALLISTIC DEPOSITION IN ONE-DIMENSIONAL SUBSTRATES

We simulated ballistic deposition in one-dimensional substrates of lengths  $L=2^n$ , with integer  $6 \leq n \leq 14$  ( $64 \leq L \leq 16384$ ). For each length  $L \leq 1024$ , two independent sets with  $10^4$  different deposits were generated, and very long steady-state regions (of interface width saturation) were observed. For each length  $L \geq 2048$ , one set with  $10^4$  different deposits was generated, but long steady-state regions were obtained only for  $L=2048$  and  $4096$ .  $W$  and  $\xi$  data were typically stored after deposition of  $L$  particles.

The interface width  $W$  as a function of time  $t$  (number of deposited particles per lattice column), for several lengths  $L$ , is shown in Fig. 1. For very short times (typically  $t \lesssim 10$ ), there is a transient region where the initial deposit is formed. In this region,  $W$  rapidly increases. After this transient, the growth region begins [Eq. (5)]; then a crossover region is observed, and finally the interface width saturates at the steady-state region [Eq. (4)].

The first step of our analysis is to propose a precise definition of the growth region. Figure 1 suggests that the linear regions of  $\log_{10}W$ -vs- $\log_{10}t$  plots have increasing declivities for increasing  $L$ , which indicates the presence of finite-size corrections to Eq. (5). Then, for fixed  $L$ , we calculated the linear correlation coefficients  $r$  of  $\log_{10}W$ -vs- $\log_{10}t$  plots using data in intervals  $t_0 \leq t \leq \tau$ , with fixed  $t_0=50$  and varying

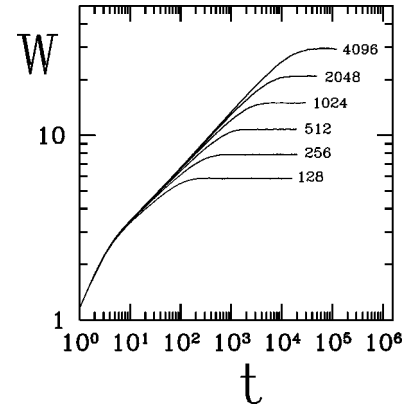


FIG. 1. Interface width  $W$  [Eq. (1)] of one-dimensional ballistic deposits as a function of time  $t$  for various lengths  $L$ .

$\tau$  (in  $t_0=50$  the average height of the porous deposit is  $h_0 \approx 100$ ). If  $\tau$  is small,  $r$  is very near 1, indicating that the data lie in an almost perfect straight line. For large  $\tau$  ( $\tau \gg t_0$ ),  $r$  typically decreases with  $\tau$ , because the  $\log_{10}W$ -vs- $\log_{10}t$  curve acquires a downward curvature (Fig. 1). Then, the condition  $r=r_{min}$  is suitable to determine the end of the growth region ( $\tau=\tau_{max}$ ) if  $r_{min}$  is high enough to ensure that all data in  $t_0 \leq t \leq \tau_{max}$  lie approximately in a straight line. In order to choose a reliable value of  $r_{min}$ , we analyzed three candidates:  $r_{min}=0.99995$ ,  $0.9999$ , and  $0.999$ . In Fig. 2 this procedure is illustrated for  $L=2048$ : visual inspection suggests linear behavior of  $\log_{10}W$ -vs- $\log_{10}t$  in the regions with  $r_{min}=0.99995$  and  $r_{min}=0.9999$ , while deviations appear for  $r_{min}=0.999$ . The same behavior is observed for other lengths  $L$ .

Effective exponents  $\beta_L$  were calculated from least squares fits of  $\log_{10}W$ -vs- $\log_{10}t$  plots using all data in the growth regions ( $t_0 \leq t \leq \tau_{max}$ ) (see Fig. 2). The results obtained from plots of  $W$  and  $\xi$  and using the above values of  $r_{min}$  are shown in Table I. Note that  $r_{min}=0.99995$  and  $0.9999$  provide nearly the same  $\beta_L$ . This analysis justifies our final

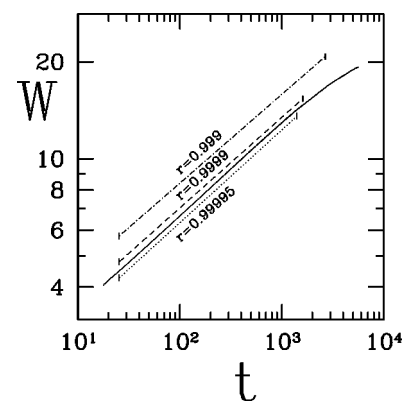


FIG. 2. The solid line shows the interface width  $W$  [Eq. (1)] of one-dimensional ballistic deposits as a function of time  $t$  for  $L=2048$ . Dashed, dotted, and dash-dotted lines have the declivities of the linear fits of the regions involved, starting at  $t_0=50$ . Those declivities are estimates of  $\beta_L$ . The linear correlation coefficient  $r$  of the data inside each region is also shown.

TABLE I. Effective exponents  $\beta_L$  in  $d=1$ , obtained from log-log plots of the quantities  $W$  and  $\xi$  and using three values of linear correlation coefficients  $r_{min}$  to determine the growth region.

$L$	$r_{min} =$	0.999	0.9999	0.999 95	0.999	0.9999	0.999 95
	Quantity:	$W$	$W$	$W$	$\xi$	$\xi$	$\xi$
256		0.2312	0.2530	0.2545	0.2388	0.2594	0.2615
512		0.2484	0.2641	0.2669	0.2541	0.2678	0.2706
1024		0.2620	0.2758	0.2778	0.2672	0.2793	0.2813
2048		0.2757	0.2869	0.2882	0.2800	0.2911	0.2924
4096		0.2837	0.2961	0.2974	0.2877	0.3001	0.3013
8192		0.2932	0.3033	0.3049	0.2967	0.3056	0.3076
16 384		0.3077	0.3099	0.3121	0.3118	0.3119	0.3139

choice  $r_{min}=0.9999$ , which will be used in the rest of this paper to determine the growth regions and to estimate  $\beta_L$ .

Following the above criteria, well defined growth regions were observed only in lattices with  $L \geq 256$ . It is also relevant to mention that we calculated  $\beta_L$  in the two independent sets of data for  $L \leq 1024$  and obtained the same estimates up to three decimal places.

Different values of  $\beta_L$  are obtained from  $W$  and  $\xi$  (see Table I). However,  $\beta_L$  has a much more remarkable variation with  $L$ , particularly for the shortest lengths. It proves that careful extrapolations of these effective exponents are necessary to calculate the asymptotic  $\beta$ . Then we propose a simple scaling form for  $\beta_L$ ,

$$\beta_L \approx \beta + AL^{-\lambda}, \quad (7)$$

where the exponent  $\lambda$  is related to corrections to scaling in Eq. (5), and  $A$  is constant.

In Fig. 3(a) we show  $\beta_L$  vs  $L^{-\lambda_1}$ , with  $\beta_L$  obtained from  $W$  and  $\lambda_1=0.28$ . This value of  $\lambda_1$  provides the best linear fit of the last five points (larger  $L$ ), and the asymptotic estimate is  $\beta=0.339$ . In Fig. 3(b) we show  $\beta_L$  vs  $L^{-\lambda_2}$  for  $\lambda_2=0.39$ , with  $\beta_L$  obtained from  $\xi$ . The same criteria was used to choose this value of  $\lambda_2$ , and the estimate  $\beta=0.328$  is obtained.

Slightly different values of exponent  $\lambda$  provide asymptotic estimates exactly equal to the KPZ value  $\beta=1/3$ :  $\lambda_1=0.32$  ( $W$ ) and  $\lambda_2=0.33$  ( $\xi$ ). The corresponding  $\beta_L$ -vs- $L^{-\lambda}$  plots are shown together in Fig. 4. The linear fits in Fig. 4 are also reliable, indicating that the exponent  $\beta$  of BD is the same of the KPZ universality class within good

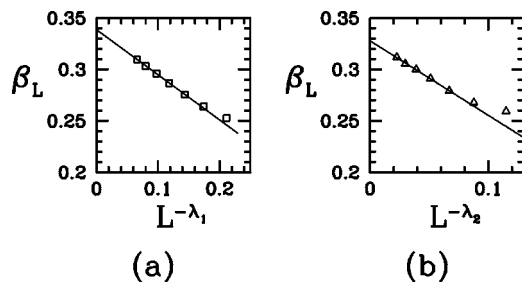


FIG. 3. Effective exponents  $\beta_L$  in  $d=1$ , obtained from log-log plots of (a)  $W$  ( $\lambda_1=0.28$ ) and (b)  $\xi$  ( $\lambda_2=0.39$ ). Straight lines are least squares fits of the last five points of each set of data.

numerical accuracy. Moreover, our analysis shows corrections to scaling in the form of Eq. (7) with  $0.2 \leq \lambda \leq 0.4$  (Fig. 4 strongly suggests speculating that  $\lambda=1/3$ ).

Now we turn to a calculation of exponent  $\alpha$ . In the steady-state region, the distributions of interface widths are very large [17]. Then we had to compute averages over many different deposits and many different times to obtain estimates of  $W_\infty(L)$  and  $\xi_\infty(L)$  with an accuracy near 0.2%. It was also necessary to compute those quantities over different ranges of  $t$  to ensure that they are fluctuating around average values and not increasing systematically with  $t$ ; the latter possibility would suggest that the steady-state region was not yet attained. Consequently, saturation widths were estimated only for  $L \leq 4096$  (at this point it is important to recall that the length of the steady-state region is not properly appreciated in  $\log_{10}W$ -vs- $\log_{10}t$  plots; that is the case for  $L=2048$  and  $L=4096$  in Fig. 1). Our estimates of  $W_\infty(L)$  and  $\xi_\infty(L)$  are shown in Table II.

We calculated effective exponents  $\alpha_L$  defined as

$$\alpha_L = \frac{\ln[W_\infty(L)/W_\infty(L/2)]}{\ln 2} \quad (8)$$

(analogously for  $\xi$ ).  $\alpha_L$  also has a remarkable dependence on  $L$ ; then a systematic extrapolation of these effective exponents is also necessary. We propose the scaling form

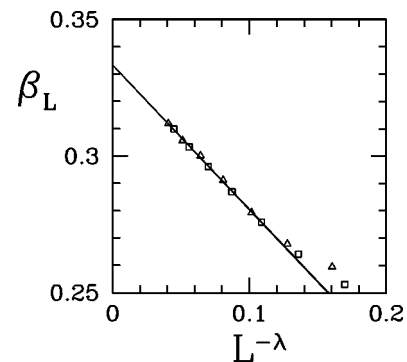


FIG. 4. Effective exponents  $\beta_L$  in  $d=1$ , obtained from plots of  $W$  (squares) and  $\xi$  (triangles), with  $\lambda=0.32$  for  $W$  and  $\lambda=0.33$  for  $\xi$ . Straight lines are least squares fits of the last five points of each set of data.

TABLE II. Estimates of interface widths  $W_\infty(L)$  and  $\xi_\infty(L)$  of one-dimensional ballistic deposits in the steady-state region (interface width saturation).

$L$	$W_\infty(L)$	$\xi_\infty(L)$
32	$3.3992 \pm 0.0069$	$3.5340 \pm 0.0074$
64	$4.4132 \pm 0.0077$	$4.5679 \pm 0.0087$
128	$5.8317 \pm 0.0108$	$6.0384 \pm 0.0119$
256	$7.8592 \pm 0.0146$	$8.1533 \pm 0.0167$
512	$10.7732 \pm 0.0236$	$11.1989 \pm 0.0247$
1024	$14.9470 \pm 0.0282$	$15.5661 \pm 0.0298$
2048	$20.9306 \pm 0.0320$	$21.8139 \pm 0.0328$
4096	$29.4140 \pm 0.0610$	$30.6819 \pm 0.0700$

$$\alpha_L \approx \alpha + BL^{-\Delta}, \quad (9)$$

where  $\Delta$  is another correction-to-scaling exponent, and  $B$  is a constant.

In Fig. 5(a) we show  $\alpha_L$  vs  $L^{-\Delta_1}$  for  $\Delta_1=0.58$ , with  $\alpha_L$  obtained from  $W_\infty(L)$ . In Fig. 5(b) we show  $\alpha_L$  vs  $L^{-\Delta_2}$  for  $\Delta_2=0.62$ , with  $\alpha_L$  obtained from  $\xi_\infty(L)$ . Those values of  $\Delta_1$  and  $\Delta_2$  provide the best linear fits of the last five points (larger  $L$ ). The asymptotic estimates obtained from the linear fits in Figs. 5(a) and 5(b) are  $\alpha=0.507$  ( $W$ ) and  $\alpha=0.506$  ( $\xi$ ), both very near the KPZ value  $\alpha=0.5$ .

The exact KPZ value is obtained if slightly different correction-to-scaling exponents are used to extrapolate the data:  $\Delta_1=0.72$  for  $W$  and  $\Delta_2=0.75$  for  $\xi$ . The  $\alpha_L$ -vs- $L^{-\Delta}$  plots have no remarkable difference from those in Figs. 5(a) and 5(b), similarly to the previous analysis of exponent  $\beta$ . Then our results show that exponent  $\alpha$  for BD is also consistent with the KPZ value, and suggests corrections to scaling [Eq. (9)] with  $0.6 \leq \Delta \leq 0.8$ .

### III. BALLISTIC DEPOSITION IN TWO-DIMENSIONAL SUBSTRATES

We simulated ballistic deposition in two-dimensional square substrates ( $L \times L$ ), with lengths  $L=2^n$ , for an integer  $4 \leq n \leq 10$  ( $16 \leq L \leq 1024$ ). For each  $L \leq 256$ , two independent sets with  $10^4$  different deposits were generated. For  $L=512$ ,  $4 \times 10^3$  different deposits were generated and, for  $L=1024$ , 100 different deposits were generated.

We did not estimate effective exponents  $\beta_L$  in these sys-

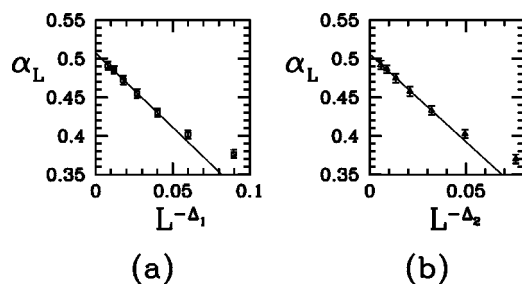


FIG. 5. Effective exponents  $\alpha_L$  in  $d=1$ , obtained from plots of (a)  $W$  ( $\Delta_1=0.58$ ) and (b)  $\xi$  ( $\Delta_2=0.62$ ). Straight lines are least squares fits of the last five points of each set of data.

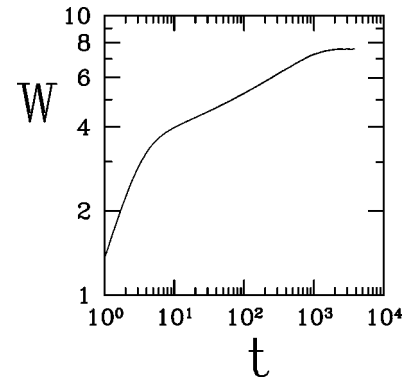


FIG. 6. Interface width  $W$  [Eq. (1)] of two-dimensional ballistic deposits as a function of time  $t$  for  $L=512$ .

tems because we could not define the growth regions, even in large lattices. In Fig. 6 we show  $\log_{10}W$  vs  $\log_{10}t$  for  $L=512$ . There is a transient region until  $t \sim 10$ , similar to the case  $d=1$ , in which  $W$  rapidly increases. From  $t \sim 10$  to  $t \sim 100$ , the average declivity in Fig. 6 decreases. However, that declivity increases again from  $t \sim 100$  to  $t \sim 1000$ , and then the crossover region begins. Consequently we did not obtain high linear correlation coefficients ( $r \geq 0.9999$ ) in any significantly large range of  $t$ , which would be essential to calculate  $\beta_L$ .

On the other hand, we were able to estimate  $\alpha_L$  [Eq. (8)] using the same methods of Sec. II. In Fig. 7(a) we show  $\alpha_L$  vs  $L^{-\Delta_1}$ , with  $\alpha_L$  obtained from  $W_\infty(L)$  and  $\Delta_1=0.49$ . In Fig. 7(b) we show  $\alpha_L$  vs  $L^{-\Delta_2}$ , with  $\alpha_L$  obtained from  $\xi_\infty(L)$  and  $\Delta_2=0.51$ . These values of  $\Delta_1$  and  $\Delta_2$  provide the best linear fits of the last four points (larger  $L$ ). The dependence of  $\alpha_L$  on  $L$  is much more impressive than in  $d=1$ , and much smaller lengths  $L$  were considered. Consequently, the asymptotic estimates of  $\alpha$  are much less accurate. From the linear fits in Figs. 7(a) and 7(b), we obtain  $\alpha=0.366$  and  $0.363$ , respectively.

These estimates are smaller than the recent estimates for the KPZ universality class,  $\alpha=0.393$  [18] (numerical) and  $\alpha=0.4$  [10] (analytical). However, with suitable choices of correction to scaling exponents ( $\Delta_1=0.38$  and  $\Delta_2=0.37$ ), the suggested exact value  $\alpha=0.4$  [10] is obtained, as shown in Fig. 8. Thus our results for BD are also consistent with KPZ in  $d=2$ , with correction-to-scaling exponents  $\Delta \sim 0.4$ .

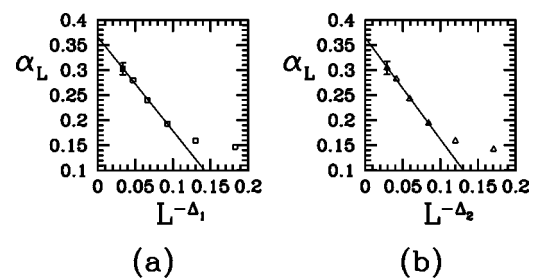


FIG. 7. Effective exponents  $\alpha_L$  in  $d=2$ , obtained from plots of (a)  $W$  ( $\Delta_1=0.49$ ) and (b)  $\xi$  ( $\Delta_2=0.51$ ). Straight lines are least squares fits of the last four points of each set of data. Error bars are smaller than the size of the symbols, except when indicated.

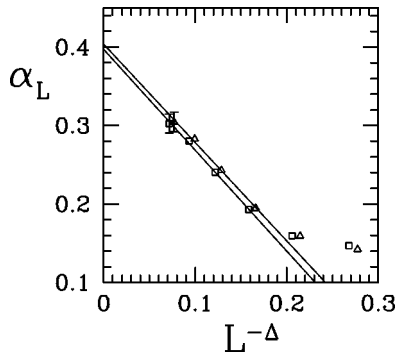


FIG. 8. Effective exponents  $\alpha_L$  in  $d=2$ , obtained from plots of  $W$  (squares) and  $\xi$  (triangles), with  $\Delta=0.38$  for  $W$  and  $\lambda=0.37$  for  $\xi$ . Straight lines are least squares fits of the last four points of each set of data. Error bars are smaller than the size of the symbols, except when indicated.

Finally, it is important to recall that the plots in Figs. 7 and 8 suggest  $\alpha > 0.35$ , while previous numerical estimates for ballistic deposition [6,13,19] were smaller than this value.

#### IV. DISCUSSION AND CONCLUSION

We simulated BD in  $d=1$  and 2 and calculated the interface widths  $W$  and  $\xi$  [Eqs. (1) and (2)]. Finite-size estimates of exponent  $\beta$  were obtained after the precise definition of the growth regions in  $\log_{10}W$ -vs- $\log_{10}t$  (or  $\log_{10}\xi$ -vs- $\log_{10}t$ ) plots. Finite-size estimates of the exponent  $\alpha$  were calculated using the saturation widths. In  $d=1$ , the effective exponents were extrapolated and gave asymptotic estimates of  $\beta$  and  $\alpha$  consistent with the KPZ universality class. Those extrapolations suggested strong corrections to scaling in this problem. In  $d=2$ , we could only estimate effective exponents  $\alpha_L$  with accuracy. The extrapolated  $\alpha$  is also consistent with recent results for the KPZ equation, and for other models that are expected to be in the same universality class. Strong corrections to scaling are also present in  $d=2$ .

Now it is essential to discuss the origin of discrepancies between previous estimates of  $\alpha$  and  $\beta$  for BD and the KPZ class. Exponent  $\beta$  is usually calculated in very large systems, where  $\log_{10}W$ -vs- $\log_{10}t$  plots show linear behavior in large intervals of time  $t$  [6,13–16]. Although different authors may consider slightly different definitions for the growth region, it does not seem that this is the origin of the discrepancies.

Indeed, our estimates of  $\beta_L$  have small differences when different linear correlation coefficients  $r_{min}$  are used to determine the end of the growth region (see the results in Table I for  $r_{min}=0.9999$  and  $0.99995$ ). Also note that our estimates are consistent with previous works. For instance, in  $d=1$ , Family and Vicsek [6] obtained  $\beta=0.30\pm 0.02$  for  $L=2000$  (to be compared with  $\beta_{2048}$  in Table I) and Halpin-Healy and Zhang [16] obtained  $\beta=0.31$  for  $L=10\,000$  (to be compared with  $\beta_{8192}$  and  $\beta_{16384}$  in Table I).

However, exponents  $\beta_L$  are not the asymptotic ones, but they are finite-size estimates that must be systematically extrapolated. The absence of those extrapolations is certainly the most important reason for the discrepancies discussed above, particularly when small lattices were considered. Our extrapolations (Figs. 3 and 4) suggest that we should work with very large lattices ( $L > 10^6$  in  $d=1$ ) to find  $\beta_L$  near the asymptotic value, using the same definition for the growth region.

Our values of  $\alpha_L$  are also consistent with previous works in  $d=1$ . For example, Family and Vicsek [6] obtained  $\alpha=0.42\pm 0.03$ , collapsing data from  $L=50$  to 500, while our data for  $64\leq L\leq 512$  give  $0.40\leq\alpha_L\leq 0.46$  [Figs. 5(a) and 5(b)]. Meakin *et al.* [13] obtained  $\alpha=0.47$  from  $\log_{10}W_\infty(L)$ -vs- $\log_{10}L$  plots using  $16 < L < 2048$ , the same value of our  $\alpha_{1024}$  (using  $L=512$  and  $L=1024$ ). D'Souza *et al.* [17] obtained  $\alpha=0.45$  from the steady-state distribution  $P(\xi)$  for  $L=127$ , while we obtained  $\alpha_{128}\approx 0.43$  (using  $L=64$  and 128) and  $\alpha_{256}\approx 0.46$  (using  $L=128$  and 256). Again we consider that the origin of discrepancies from the KPZ value is associated with the absence of extrapolations of effective exponents. Since it is very difficult to attain the steady-state regimes in very large lattices, the calculation of  $\alpha$  is restricted to relatively small  $L$  and one necessarily has to deal with strong finite-size effects.

Finally, we expect that this work will motivate further studies to explain the corrections to scaling obtained in  $d=1$ , and we suggest the application of the same methods to analyze related models, particularly in  $d=2$ , where interesting applications frequently appear.

#### ACKNOWLEDGMENTS

This work was partially supported by CNPq and FINEP (Brazilian agencies).

[1] A.-L. Barabási and H. E. Stanley, *Fractal Concepts in Surface Growth* (Cambridge University Press, New York, 1995).  
 [2] V. P. Zhdanov and P. R. Norton, *Surf. Sci.* **459**, 245 (2000).  
 [3] H. F. El-Nashar and H. A. Cerdeira, *Phys. Rev. E* **61**, 6149 (2000).  
 [4] Y. Shapir, S. Raychaudhuri, D. G. Foster, and J. Jorne, *Phys. Rev. Lett.* **84**, 3029 (2000).  
 [5] M. J. Vold, *J. Colloid Sci.* **14**, 168 (1959); *J. Phys. Chem.* **63**, 1608 (1959).

[6] F. Family and T. Vicsek, *J. Phys. A* **18**, L75 (1985).  
 [7] M. Kardar, G. Parisi, and Y.-C. Zhang, *Phys. Rev. Lett.* **56**, 889 (1986).  
 [8] J. G. Amar and F. Family, *Phys. Rev. A* **41**, 3399 (1990).  
 [9] K. Moser, J. Kertész, and D. E. Wolf, *Physica A* **178**, 215 (1991).  
 [10] M. Lässig, *Phys. Rev. Lett.* **80**, 2366 (1998).  
 [11] J. M. Kim and J. M. Kosterlitz, *Phys. Rev. Lett.* **62**, 2289 (1989).

- [12] T. Nagatani, Phys. Rev. E **58**, 700 (1998).
- [13] P. Meakin, P. Ramanlal, L. M. Sander, and R. C. Ball, Phys. Rev. A **34**, 5091 (1986).
- [14] P. Meakin, Phys. Rep. **235**, 189 (1993).
- [15] R. M. D'Souza, Int. J. Mod. Phys. C **8**, 941 (1997).
- [16] T. Halpin-Healy and Y.-C. Zhang, Phys. Rep. **254**, 215 (1995).
- [17] R. M. D'Souza, Y. Bar-Yam, and M. Kardar, Phys. Rev. E **57**, 5044 (1998).
- [18] E. Marinari, A. Pagnani, and G. Parisi, J. Phys. A **33**, 8181 (2000).
- [19] R. Baiod, D. Kessler, P. Ramanlal, L. Sander, and R. Savit, Phys. Rev. A **38**, 3672 (1988).